Novel CellCage™ technology integrates image-based phenotyping and single-cell transcriptomics to study dynamic behaviors of living cells

Frank Charbonier[1], Yunmin Li[1], Nick Elder[1], Olaia Vila[1], Sina Farahvashi[1], Shreya Deshmukh[1], Mehdi Mohseni[1], Camilla Valente[2], Justin Poelma[1], Nirvan Rouzbeh[1], Elaheh Farjami[1], Meng Taing[1], Mika Maenaga[1], Teresa Ai[1], Shan Sabri[1], Liz Wu[1], Pier Federico Gherardini[1], Sina Moeinzadeh[1], Matthew Spitzer[2], Tarun Khurana[1], Gary Schroth[1], Mostafa Ronaghi[1]

[1]Cellanome, Foster City, CA [2]Dept. of Otolaryngology-Head and Neck Surgery, UCSF School of Medicine, San Francisco, CA

ABSTRACT Imaging-based technologies are widely used to study cellular phenotypes in vitro because they provide multi-modal readouts of morphological, molecular, and functional cell states. However, integrated technologies which can directly link dynamic behaviors of living cells with high quality transcriptomic data at single-cell resolution are lacking. To address these limitations, **we developed a novel CellCage™ Enclosure (CCE) technology: biocompatible and degradable hydrogel microenvironments** formed by light-guided polymerization around individual cells or defined groups. CCEs enable long term culture of tens of thousands of cells, longitudinal imaging of dynamic cell behaviors, and direct mapping of image-based phenotypes to transcriptomic profiles on Cellanome's R3200 platform. In contrast to standard well plate, nanowell, or droplet-based methods, the properties of CCEs (i.e., size, shape, location, porosity, substrate) can be configured depending on the cell and assay type. CCEs can be formed on the order of seconds and selectively degraded on the order of minutes using cell-compatible chemistry. Permeable CCE walls allow diffusion of nutrients, waste, and fluorescence reagents, enabling the culture of suspension or adherent cells for weeks.

We demonstrate CCE versatility across multiple applications. First, we correlated phagocytosis activity with transcriptomes in microglial cells, linking functional phenotypes to gene expression states. Second, we integrated image-based morphological embeddings of adherent cells with single-cell transcriptomic data to reveal functionally relevant cellular heterogeneity. Third, we co-enclosed dendritic cells with T cells to capture time-resolved activation dynamics during cell-cell interactions. Beyond these established applications, we also highlight emerging capabilities enabled by CCE technology. These include selective enrichment or selective retention of target cells from mixed populations for functional profiling, e.g., retention of CD56+ NK cells from an unlabeled PBMC cell mix. Additionally, we demonstrated integrated calcium imaging and transcriptome profiling from single astrocytes. **Together, these results demonstrate that CCE technology enables novel multi-modal measurements linking dynamic cellular behaviors, morphological phenotypes, and single-cell transcriptomics across diverse experimental contexts.**

CELLANOME'S R3200 PLATFORM LINKS IMAGE-BASED PHENOTYPING AND TRANSCRIPTOMICS

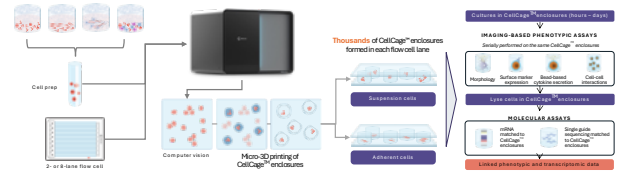

Fig 1. Schematic of Cellanome's CellCage™ technology enabling multi-modal phenotypic and functional profiling of the same cells.
Tens of thousands of suspended cells are mixed with hydrogel precursor and loaded into a multi-lane flow cell. Individual cells are located, and CellCage™ enclosures (CCEs) are automatically generated around them via light-guided polymerization. The CCEs are permeable to antibodies and small molecules, allowing long-term culture and time-course imaging of the same cells. Following imaging-based assays, cells are lysed in situ, and mRNA is captured for cDNA synthesis, library preparation, and sequencing.

BIOCOMPATIBLE CELLCAGE™ ENCLOSURES (CCEs) SUPPORT CULTURE AND PROFILING OF DIVERSE CELL TYPES

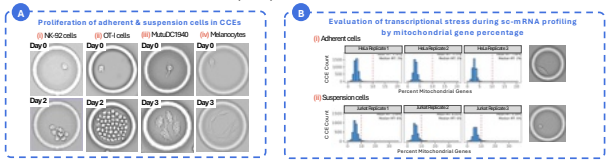

Fig 2. CCE biocompatibility maintains cell viability.
(A) CCEs support viability and proliferation for a wide range of cell types. (B) Evaluation of transcriptional stress in sc-mRNA runs on Cellanome platform by mitochondrial (MT) gene %. Three independent replicates each, with one replicate per lane, for (i) HeLa cells with adherent workflow and (ii) with Jurkat cells for suspension workflow show median MT% ~3% and ~6%, respectively, indicating low cell stress. Brightfield images shows example CCEs before cell lysis.

PERMEABLE CCE WALLS ALLOW DELIVERY OF SMALL MOLECULES AND FLUORESCENT REAGENTS

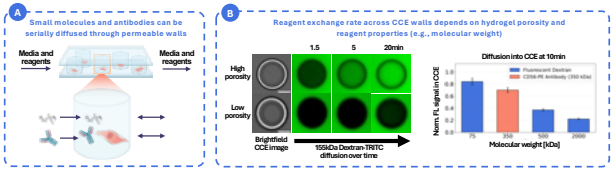

Fig 3. Reagent exchange through porous walls of CellCage™ Enclosures (CCE).
(A) Permeable CCE walls allow diffusion of nutrients, waste, and fluorescence reagents, enabling long-term cell culture. (B) Reagent exchange rate depends on hydrogel porosity and properties of the diffusing reagent (e.g., molecular weight). Brightfield and fluorescence images show 155kDa Dextran-TRITC diffusion through high vs low porosity CCE walls over 20 minutes. Scalebars, 50μm. Bar graph shows fl. signal within CCEs normalized to signal outside of CCEs at 10 minutes for fluorescent dextrans (75, 500, 2000 kDa) and CD56-PE antibody (~350 kDa). Diffusion inversely correlates with molecular weight.

FLEXIBLE CELLCAGE™ ENCLOSURE CONFIGURATIONS ENABLE DIVERSE WORKFLOWS

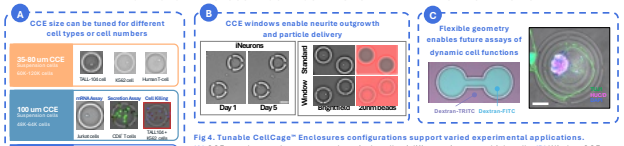

Fig 4. Tunable CellCage™ Enclosures configurations support varied experimental applications.
(A) CCEs can be tuned to accommodate single cells of different sizes or multiple cells. (B) Window CCEs feature configurable openings to permit neurite outgrowth while maintaining cell enclosure. Scalebar, 50μm. Windows enable selective particle delivery; images show 20 nm FluoSpheres™ (red) entering CCEs with 5μm windows while cells remain enclosed. (C) Light-guided polymerization enables flexible geometries for specialized assays. Dumbbell CCE illustrates spatial compartmentalization of Dextran-FITC (cyan) and Dextran-TRITC (magenta). Maze CCE allows spatially restricted neurospheres to contact for neurite pathfinding studies. Scalebar, 130μm.

CELLCAGE™ ENCLOSURES ENABLE DIVERSE IMAGE-BASED PHENOTYPING ASSAYS

PHAGOCYTOSIS ASSAY ON MICROGLIAL CELLS

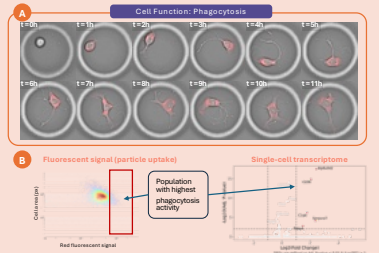

Fig 5. Correlation of phagocytosis activity and transcriptome on BV2 microglial cells.
(A) Time-lapse of a single BV2 microglial cell phagocytosing pHrodo™ BioParticles™. CellCage™ enclosures were formed around single microglial cells in the presence of red E. coli pHrodo BioParticles. Images were acquired every hour over a 12h period. Increase of red signal shows phagocytosis of the particles. (B) High-throughput analysis of phagocytosis activity and single-cell transcriptome. Microglial cells with the highest phagocytosis activity show overexpression of genes related to phagocytosis and complement signaling (Cd36, C1qb), lipid transport and oxidative stress regulation (Serpina7, Fabp4) and lysosomal function (Atp6v0d2).

INTEGRATING MORPHOLOGICAL FEATURES WITH TRANSCRIPTOMIC PROFILES OF ADHERENT CELLS

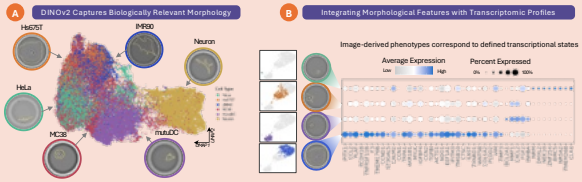

Fig 6. DINOv2: a self-supervised model for extracting morphological features from images.
(A) DINOv2 features from six cell lines clustered by cell identity, confirming capture of meaningful morphological differences. Embedding similarity predicted the generalization performance of a Mask R-CNN (Region-based Convolutional Neural Network) segmentation model. (B) Clustering of DINOv2 features from fibroblast CCE images identified four distinct morphological states — ranging from fully adhered, ECM3-enriched cells (CCN2, ST3GAL5; Blue cluster) to weakly adhered, inflammatory cells (CXCL2, MMP1; Orange cluster), with intermediate adhesion-stress profiles. These morphology-defined phenotypes were undetectable by transcriptomic clustering alone, demonstrating that image-derived embeddings capture functionally relevant cellular heterogeneity.

CELL-CELL INTERACTIONS: T-CELL PRIMING BY SINGLE DENDRITIC CELLS

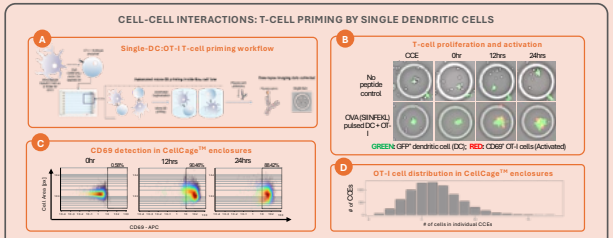

FIGURE 7: Establishing T-cell priming assay with single dendritic cells using Cellanome's R3200.
(A) MutuDC1940 cells are loaded onto the flow cell and pulsed with OVA peptide. Primary mouse OT-I cells mixed with hydrogel precursor are loaded, followed by encapsulation of single DCs with OT-I cells in CCEs. Time-lapse imaging evaluates T-cell proliferation (brightfield cell counts) and activation via fluorescent detection of CD69/CD71 expression. (B) Imaging of single MutuDC1940 cells with OT-I cells in CCEs at different timepoints. (C) Successful OT-I priming by individual DCs indicated by increased percentage of CCEs positive for CD69 from 0 to 24 hours. Each dot represents average CD69 signal by all cells in a single CCE, quantified for >7000 CCEs. (D) Distribution of CCEs by number of enclosed OT-I cells, enabling normalization of DC priming analysis to starting OT-I cell number at d0.

CELLCAGE™ ENCLOSURE-ENABLED WORKFLOWS IN DEVELOPMENT

SEQUENTIAL ENRICHMENT OF RARE CELLS FROM MIXED POPULATION FOR CYTOKINE PROFILING

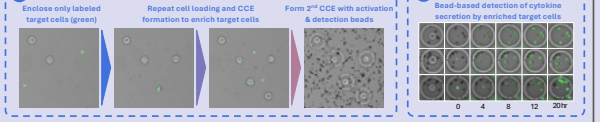

Fig 8. Sequential enrichment of CD8+ CAR T cells from PBMCs enables functional cytokine profiling.
(A) Pre-activated CD8+ T-cells (green) were spiked into PBMCs at 5% and subjected to iterative rounds of CCE formation to enrich the target population. Following three rounds of fluorescence-guided selective enclosure, a fourth CCE formation step with a second gel type introduced activation and cytokine detection beads alongside the enriched CD8+ T-cells. (B) Following degradation of the first gel type, the enriched CD8+ T-cells were monitored for IFNγ secretion and proliferation.

SELECTIVE RETENTION OF TARGET CELLS FROM MIXED POPULATION FOR FUNCTIONAL PROFILING

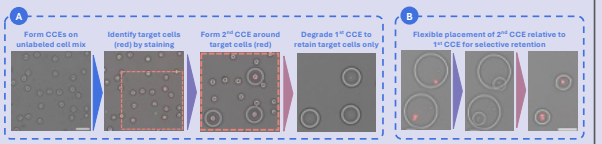

Fig 9. Selective retention of NK cells from mixed PBMC population via sequential CCE formation.
(A) Peripheral blood mononuclear cells (PBMCs) were initially enclosed in small CCEs. Scalebar, 100μm. PBMCs were stained with fluorescent antibodies to identify NK cells (CD56+, red) and B cells (CD19+, green). NK cells were targeted for secondary CCE formation with a larger CCE size and a different gel type. The first round of small CCEs were selectively degraded to retain only the CD56+ NK cells for further analysis. (B) Orthogonal degradation of different gel types enables flexible selective retention strategies. The relative size and placement of the 1st and 2nd CCEs can be configured to accommodate different experimental designs. Images from a separate experiment. Scalebar, 100μm.

INTEGRATED CALCIUM IMAGING AND TRANSCRIPTOME DATA FROM SINGLE ASTROCYTES

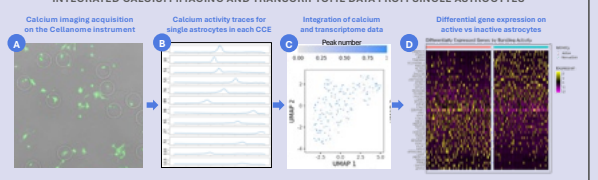

Fig 10. Acquisition of calcium imaging and transcriptome data from single astrocytes in CCEs.
(A) iPSC-derived astrocytes were enclosed in CCEs and imaged using Fluo4-AM calcium dye. Each FOV was imaged at 1.3 Hz for 5 minutes. (B) Calcium imaging data was processed to extract activity traces for single astrocytes in each CCE. (C) After calcium activity was measured, scRNA-seq data was collected from the same single cells, enabling linked scRNA-seq and calcium activity data to be collected from the same cell. (D) Differential gene expression analysis was performed comparing active vs inactive astrocytes.

CELLCAGE™ ENCLOSURES: CONFIGURABLE MICROENVIRONMENTS

ENABLING MUTLTI-MODAL MEASUREMENTS FROM LIVING CELLS OVER TIME